UNSUPERVISED IMAGE ENDMEMEBER DEFINITION IN MULTISENSOR IMAGE DATA

A. Greiwe

University of Osnabrueck, Institute for Geoinformatics and Remote Sensing (IGF), Osnabrueck, Germany - agreiwe@igf.uni-osnabrueck.de

KEY WORDS: Imaging spectroscopy, Endmember selection, Urban monitoring

ABSTRACT:

In a recent studie (Greiwe and Ehlers, 2005), the author developed a decision based data fusion approach for the analysis of spatial and spectral high resolution image data of an urban scene. Image segments of high resolution orthophotos were classified with additional material information derived from hyperspectral image data. To retrieve this material information, the hyperspectral image data were classified by the Spectral Angle Mapper (SAM). Results of SAM were included into the classification of the high resolution orthophotos. The inclusion of hyperspectral image data significantly increased the classification accuracy of a high resolution orthophoto.

One of the steps of the data fusion approach described above that more often requires the user input , is the SAM classification of hyperspectral data. One of the preconditions for the analysis of hyperspectral image data is the definition of a set of material reference spectra – often called image endmember. A manual selection of image pixel as a definition of image endmember leads to user dependent results. To avoid this, many approaches for unsupervised image endmember definitions, such asPPI or N-FINDR (Winter 1999) have been developed. These algorithms detect those pixels that define the convex hull of the n-dimensional feature space of hyperspectral image data. This produces endmembers that express ‘spectral extreme’ features. Although the resulting endmembers are useful for spectral unmixing approaches, they are not suitable for material detection approaches like SAM. Algorithms like SAM, determine the spectral similarity between a pixel’s spectra and a given endmember. In contrast to endmembers that are defined by ’spectral extremes’, SAM needs endmembers that represent mean spectra of material types in order to produce best possible results between spectrally similar material classes.

The objective of this work is the development and implementation of a unsupervised image endmember definition approach for material detection methods like SAM. Information on the high spatial resolution orthophoto is used to detect homogeneous areas in the hyperspectral image data. Pixels of the hyperspectral image data in such homogenous areas are marked as endmember candidates. Then, a spectral correlation analysis (van der Meer and Bakker 1997) is used to calculate the spectral similarity between the candidates. At n given candidates, the n*n correlation matrix of all candidates is introduced as a new feature space that expresses spectral similarity between the candidates. Candidates with similar spectral behavior are grouped by a density based cluster algorithm. The mean spectrum of each cluster is stored in a spectral library for further processing. In an urban test site, several endmember for different materials could be defined by the proposed approach.

1. INTRODUCTION

Hyperspectral image data contains a large number of narrow bands that form a high dimensional “image data cube”. To process this large amount of data, special classification algorithms for spectral unmixing or for material detection have been developed. Material detection algorithms like the Spectral Angle Mapper (SAM) calculate a deterministic value to express the spectral similarity of a pixel to a given reference. Unmixing approaches like the Mixture Tuned Matched Filtering (MTMF) determine for a measured spectrum the abundance fraction of a given reference spectrum. In both cases, the term “endmember” is used for the spectral reference definition.

The definition of endmembers should be carried out taking into account their intended use. Endmembers obtained by a given approach may not be useful for both material detection algorithms (e.g. SAM) or for unmixing analyses (e.g. MTMF). For unmixing approaches, several manual or unsupervised endmember selection methods such as the Manual Endmember Selection Tool (MEST) (Bateson and Curtis 1998), the Pixel Purity Index (PPI), implemented in ENVI (Boardman et al. 1995), or the NFINDR (Winter 1999), have been developed. These well-known algorithms detect those pixels in hyperspectral image data that define the convex hull of a point cloud in the corresponding spectral n-dimensional feature space.

Algorithms for material detection purposes, like SAM, determine the spectral similarity between a pixel’s spectra and a given endmember. In contrast to endmembers for spectral unmixing, which often represent ’spectral extreme’ features, algorithms like SAM require endmember containing the ‘mean spectrum’ of a material class in order to produce the best possible results between classes with a similar spectral behaviour. The determination of reference spectra as an endmember for material detection approaches like SAM could be carried out by measurements *in situ* with a field spectrometer or by a selection of pixels in the image data. The objective of this work is the development and implementation of an un supervised image endmember definition approach.

2. METHODS

2.1 Determination of Endmember Candidates

As a first step of this approach, all candidate pixels for image endmembers, have to be determined. A pixel in the hyperspectral data that contains the reflectance spectrum of a homogenous surface is a candidate for a material definition. Due to the relatively coarse spatial resolution of imaging spectrometers (e.g. ground sampling distance of > 3 m), many pixels contain mixed spectra. These pixels are mostly located at the intersection of two surfaces with different spectral features. If the geometry of these objects is known, these mixed pixels could be filtered out and disregarded in further processing. In a multisensor environment, spatial high resolution image data could be segmented in order to retrieve this necessary geometry information. In this study, the image segments were derived by use of a region growing segmentation technique, the Fractal Net Evaluation Approach (FNEA) (Baatz abd Schäpe 1999, eCognition software), from an digital orthophoto (0.25 m ground sampling distance).
After superimposing the image segments of the orthophoto on the hyperspectral image, pixels completely (within N4 or N8 neighborhood, see figure. 1) included in these segments were chosen as candidates for an endmember definition.

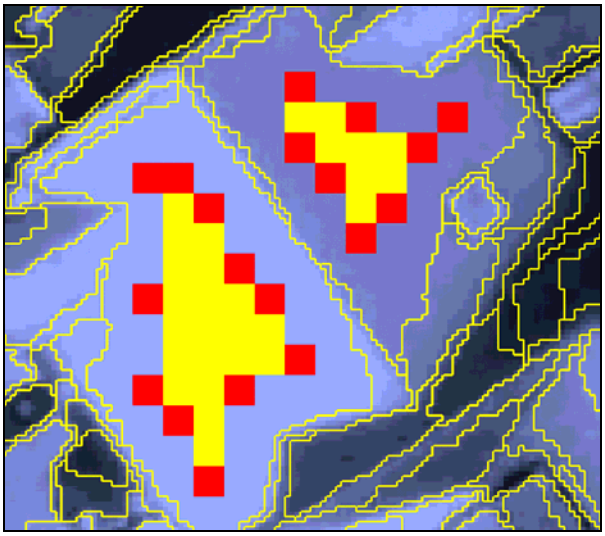

Figure 1: Segments (yellow lines) of an orthophoto (shown as blue background) are used to determine candidate pixel in the hyperspectral image data. N8-filtered candidates are shown in yellow, N4-filtered, in red.

Then, the endmember candidates pixels were grouped according to similar spectral characteristics. The geometric information (link between candidate and segment) is not used in the following approach. As a consequence, invalid image segments containing different material spectra have no influence on the following definition process.

2.2 Measuring spectral similarity

Endmember candidates were clustered by their spectral similarity using a distance based approach. For this, a feature space to determine the proximity matrix between all objects to be clustered was developed In a first approach, the original spectral feature space was taken into account. However, often in urban settings the spectra of reference materials are in turna result of a spectral mixture of different (man-made) materials. As a result, this mixture leads to flat spectra without distinct material specific spectral charateristics. In addition, some of these materials have similar spectral features and are hardly separable in an original or transformed feature space, as shown in figure 2.

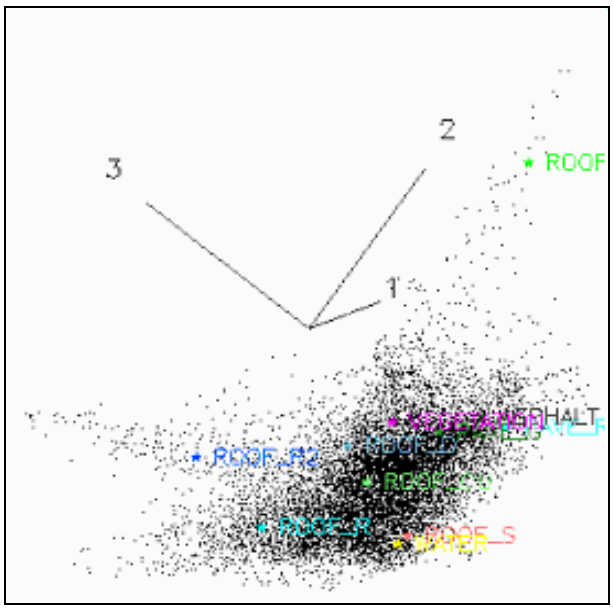

Figure 2: Image endmembers of urban materials in a MNF feature space (first three axes of MNF feature space). Reference pixel of mixed materials are mostly located in the center of the point cloud.

Deterministic approaches like SAM allow the construction of an advanced feature space for the separation of spectrally similar candidates. The image spectra of all candidates can be stored in a binary array and afterwards classified with SAM. The reference spectra for this classification step is the spectrum of the first candidate. For example, a group of 23 candidates will lead to 23 spectral angles (result of SAM) for each candidate. This leads to a matrix as shown in figure 3. Here, the spectral angle was calculated for each candidate with respect to the other 22 candidates. The SAM matrix in Figure 3 shows distinct groups of candidates with similar SAM angles.

1	0,00	0,11	0,03	0,70	0,69	0,69	0,69	0,53	0,54	0,53	0,53	0,40	0,40
2	0,11	0,00	0,13	0,72	0,71	0,71	0,71	0,55	0,55	0,55	0,54	0,40	0,40
3	0,03	0,13	0,00	0,69	0,69	0,69	0,69	0,53	0,53	0,53	0,53	0,40	0,40
4	0,70	0,72	0,69	0,00	0,00	0,01	0,01	0,18	0,18	0,18	0,18	0,34	0,34
5	0,69	0,71	0,69	0,00	0,00	0,01	0,00	0,17	0,17	0,17	0,18	0,33	0,34
6	0,69	0,71	0,69	0,01	0,01	0,00	0,01	0,18	0,17	0,17	0,18	0,34	0,34
7	0,69	0,71	0,69	0,01	0,00	0,01	0,00	0,17	0,17	0,17	0,18	0,33	0,34

Figure 3: First seven Rows of a matrix with spectral angles. Row one, column two is the angle (value = 0,11) between candidate one and candidate two. Distinct groups of candidates are shown in color.

The matrix with the SAM-results (see figure 3) can also be viewed as a n-dimensional feature space. By representing the first row on an x-axis, the second on a y-axis and the third on a z-axis, a new feature space can be created (see figure 4).

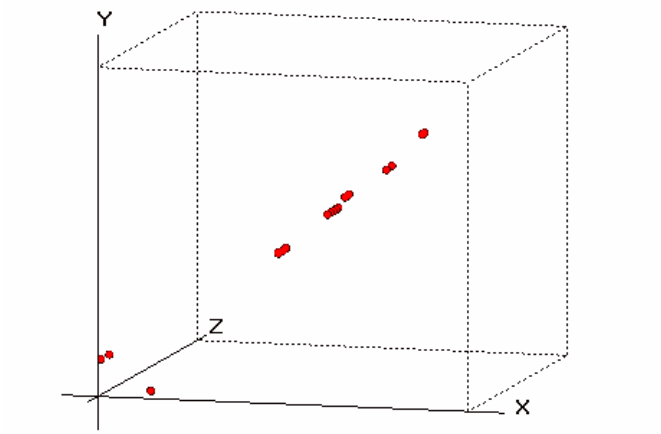

Figure 4: Three dimensional feature space produced by the rows of the SAM matrix displayed in figure 3.

The feature space in figure 4 shows seven distinct clusters due to the spectral diversity of the given material groups. The high correlation between the candidates is evident. Nevertheless, distinct groups of candidates are visible. As a result, for each material, a group of spectral similar candidates, belonging to this material, can be detected.

Taking the same material types and increasing the number of candidates, a feature space is formed like in figure 5. The deistinct groups, as shown in figure 4 are connected. A definition of seven destinct clusters is hardly possible.

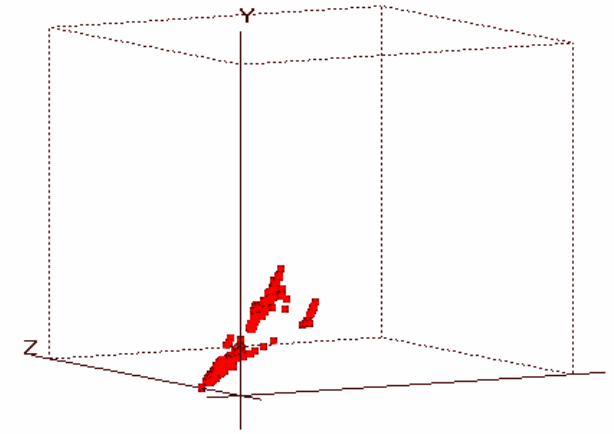

Figure 5: Three dimensional feature space, spawned by three rows of the SAM-matrix. For the displayed data, 600 candidates were processed..

The use of SAM-results to determine spectral similar groups of candidates as displayed in figure 4 and figure5 show first promising results. To improve the performance of this approach, another statistical measure is introduced in the proposed algorithm.

The correlation coefficient is another deterministic approach for the estimation of spectral similarity. The correlation coefficient allows a more precise differentiation of spectrally similar materials (Carvalho et al., 2000). This technique is also used in classification approaches like the Cross Correlogram Spectral Matching (CCSM, van der Meer and Bakker, 1997) and pattern recognition in hyperspectral image data (Ingram et al., 2004).
To estimate the spectral correlation between two given image pixels, first the sum of reflectances r_{ij} of a pixel p_j:

$$p_j = \sum_{i=1}^{n} r_{ij} \qquad (1)$$

are transformed by subtracting the mean value of rj and normalizing to one, so that the spectra have the following characteristics:

$$\sum_{i=1}^{n} a_i = 0 \qquad \sum_{i=1}^{n} a_i^2 = 1 \qquad (2)$$

The correlation coefficient could be estimated by:

$$c_j k = \sum_{i=1}^{n} a_{ij}\ a_{ik} \qquad (3)$$

The calculation of the correlation coefficient between n candidates results in a n×n correlation matrix. The rows of the correlation matrix can be used as the definition of the coordinateaxis of a new feature space (see figure 6).

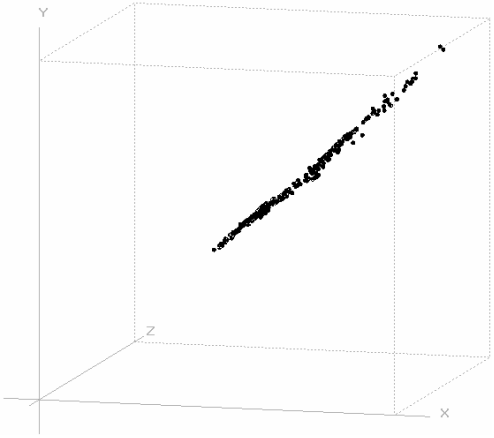

Figure 6: Rows of a correlation matrix as feature space which is highly correlated.

The first three rows of a correlation matrix of 444 candidates are displayed in Figure 6. Figure 7 shows a different selection of rows (1,3 and 13).

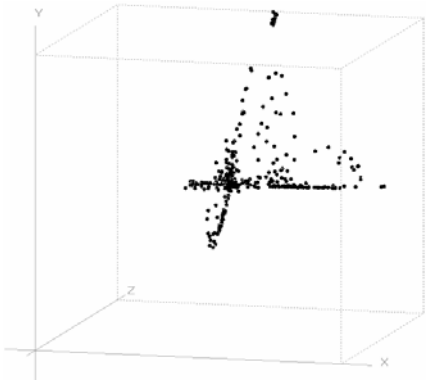

Figure 7: Rows of a correlation matrix as feature space.

The separability of candidates in the feature space is highly dependant on the selection of rows from the correlation matrix, which defines the axes of the new feature space. As a consequence, a Principal Component Analysis (PCA) is carried out within the complete correlation matrix data. The result is a PCA-transformed correlation matrix with rows sorted by the eigenvalues of the PCA. The rows of this transformed matrix can also be used as definition for the coordinate axes of an n-dimension feature space (see Figure 8).

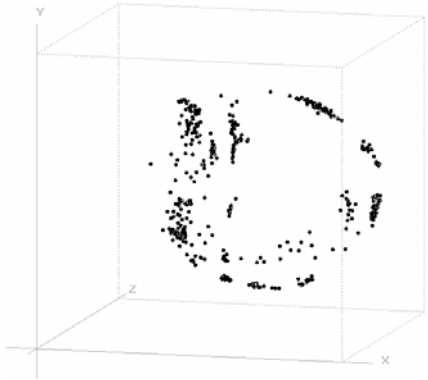

Figure 8: Feature space, resulting from a PCA-transformed correlation matrix. The first three PCAcomponents define the axes of the feature space.

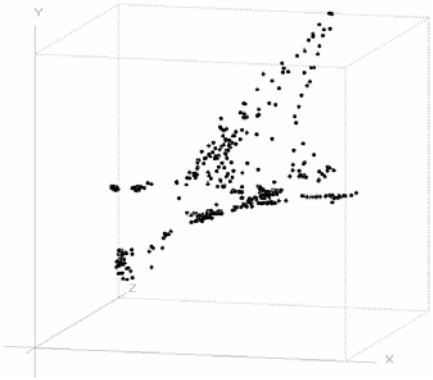

Figure 9: A combination of higher PCA components (3, 5 and 7) still shows distinct groups of spectral similar candidates.

2.3 Clustering of similar spectra

Candidates in the PCA-transformed feature space build linear point clouds (Figure 8). Clustering algorithms such as k-means or ISODATA offer no solution to separate distinct clusters from an aggregated cloud of points like the one shown in Fig. 8. Therefore, the density based clustering algorithm (also known as DBSCAN) was used here to cluster the candidates. A radius representing the neighborhood of a point is predefined by the user. This neigborhood has to contain a minimum number of points in order to build a cluster. The radius and the number of points in the given neighborhood are the two threshold values defining the 'density' of a cluster (Figure 10).

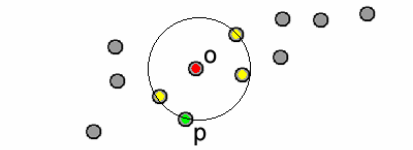

Figure 10: For a given radius and a minimum numbers of reachable neighbor points, point O is a core object of a new cluster including neighbor points like P.

In further iterations, reachable neighbors are gradually included into the cluster. Based on this strategy, point clouds with drawn-out shapes could be clustered (see figure 11).

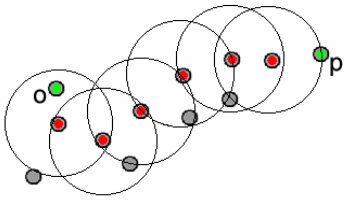

Figure 11: The points O and P belong to the same cluster, connected through the core objects (displayed in red).

For this study, the radius was estimated by the mean minimum distance to the next neighbor over all points in the dataset. The number of neighbors, was chosen to range from 1 to 3. The results of the described clustering algorithm is shown in figure 12.

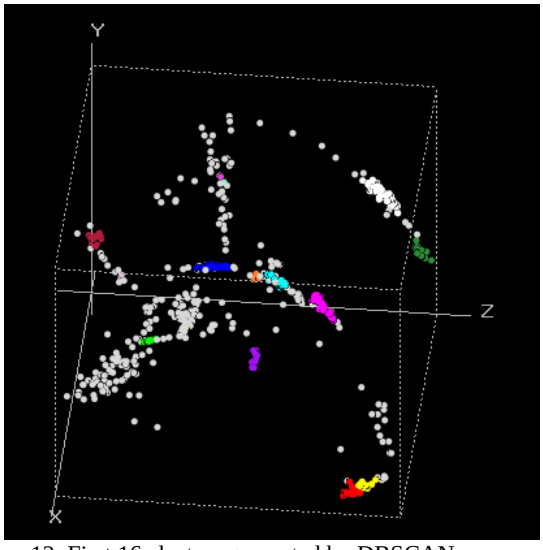

Figure 12: First 16 clusters generated by DBSCAN.

2.4 Building the spectral library

DBSCAN provides a Cluster-ID for each candidate. In case of a clustering, a candidate retrieves the ID of the assigned cluster. A negative ID (-1) indicates those candidates, who are not assigned to any cluster. As a result of the clustering process, a mask image with the same extent as the hyperspectral image data contains these cluster IDs at the geometric location of each candidate. Pixels with the same ID (member of a cluster) could be joined into one group (using a region of interest, ROI, Envi). Averaging the corresponding spectra of such a group in the hyperspectral dataset leads to a reference spectra.

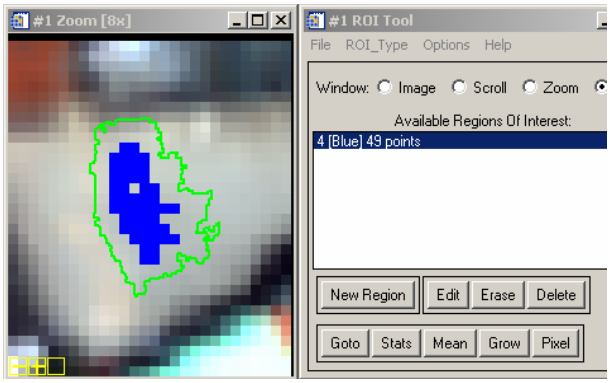

Figure 13: Image pixel, grouped by their cluster ID on the left lead to a group of 49 pixel (right).

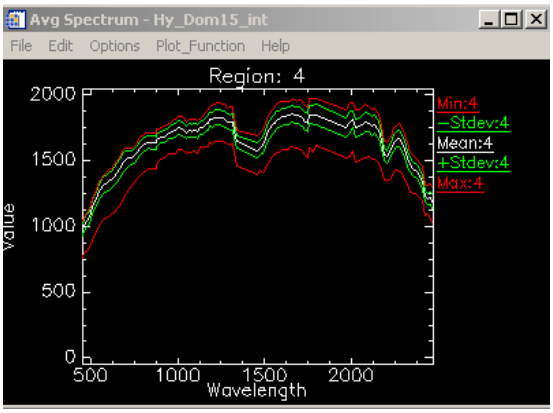

Figure 14: The average spectrum of a cluster (Fig. 13) and statistical parameters (min, max, stddev) can be estimated by use of standard software.

3. RESULTS

The proposed method was used to detect ten different known materials in an urban test site (500 m x 1000 m). After an image segmentation of an orthophoto, covering the whole scene, a subset of image segments with six known ground materials and four known roofing materials was used to estimate the set of endmember candidates. 753 candidates were detected and clustered by DBCSAN. The first 16 cluster were stored in a spectral library, the statistical properties of the reference spectra are shown in table 1.

Table 1: The first 16 clusters and their statistical properties.

Cluster	# Pixels	Standardd eviation	Material
1	101	1,1 %	Granite (pavement)
2	79	7,5 %	Clay (red roofing)
3	51	0,5 %	Granite (pavement)
4	58	5,3 %	Vegetation
5	47	11,2 %	Concrete rooftop
6	48	5,3 %	Clay (dark roofing)
7	57	4,1 %	Copper
8	59	3,8 %	Asphalt/Bitumen
9	22	16,5 %	Zinc
10	21	1,1 %	Copper
11	57	0,3 %	Water
12	16	0,5 %	Concrete
13	16	0,3 %	Clay pavement
14	10	0,3 %	Water/vegetation
15	9	4,2 %	Clay (red roofing)
16	7	0,3 %	Gravel

All ten material types known to be present in the image were included in the 16 clusters shown in Table 1 . Some material clusters like granite (clusters 1 and 3) and red clay roofing material (cluster 2 and 9) were erroneously classified as two different groups. However, the high standard deviation of some roofing materials (e.g. cluster 5 with 11,2%) shows that this method is able to correctly classify pixels of the same material with different surface slopes or aspects.

4. CONCLUSION

The presented algorithm for an unsupervised endmember selection shows first promising results. A reliable transformation method from the original spectrum to a feature space that expresses the similarity of spectra has been developed. The following density based clustering lead to useful pixel groups, which average spectra can be stored in a spectral library. Future steps will be the development of a framework application to assist the user for quality assessment and a vsiual control on the clustering process.
Finally, by use of this approach, the user has only to examine the results of the clustering process and to join some clusters manually, if necessary. The manual selection of image pixel for a certain material is replaced by this approach.

REFERENCES

Baatz, M. und Schäpe, A., 1999: Object-oriented and multi-scale image analysis in semantic networks. In: Proc. of the 2nd International Symposium on Operationalization of Remote Sensing, Enschede, ITC.

Bateson and Curtiss, 1996: A Method for manual endmember Selection and Spectral Unmixing, *Remote Sensing and Environment* (55), pp. 229–243.

de Carvalho Jr, O. A., de Carvalho, A. P. Ferreira und Meneses, P. R., 2000: Sequential mini-mum noise fraction use: An approach to noise elimination. In: Summaries of the Ninth Annual JPL Airborne Earth Science Workshop. JPL Pub 00-18.

J. W. Boardman, F. A. Kruse, and R. O. Green 1995: Mapping target signatures via partial unmixing of aviris data. In: Summaries, Fifth JPL Airborne Earth Science Workshop, JPL Pub-lication 95-1 (1), pp. 23–26.

A. Greiwe and M. Ehlers, "Combined analysis of hyperspectral and high resolution image data in an object oriented classification approach," in Proceedings of 3rd International Symposium on Remote Sensing and Data Fusion over Urban Areas 13-15 March 2005, Phoenix(Arizona), USA, 2005

Ingram, R. N., Lewis, A. S. und Tutweiler, R. L., 2004: An automatic nonliear correlation ap-proach for processing of hyperspectral images. *International Journal of Remote Sensing*, Vol 25(20): pp. 4981–4998.

F. van der Meer and W. Bakker, 1997. CCSM: Cross Correlogram spectral matching. *International Journal of Remote Sensing* 18, pp. 1197–1201.

M. E. Winter, "Fast autonomous spectral endmember determination in hyperspectral data," in Proceedings of the Thirteenth International Conference on Applied Geologic Remote Sensing, pp. 337 – 344, Volume II, Vancouver B.C., Canada, 1999